Preliminary computational study of centrifugal compressor inlet flow instabilities with radial inlet guide vanes

Cite as: AIP Conference Proceedings **2323**, 060006 (2021); https://doi.org/10.1063/5.0041454
Published Online: 08 March 2021

Lukáš Hurda, and Richard Matas

Preliminary Computational Study of Centrifugal Compressor Inlet Flow Instabilities with Radial Inlet Guide Vanes

Lukáš Hurda[1, a)], Richard Matas[2, b)]

[1]*University of West Bohemia, Faculty of Mechanical Engineering, Department of Power Systems Engineering, Univerzitní 2762/22, 301 00 Plzeň, Czech Republic*
[2]*University of West Bohemia, New Technologies – Research Centre, Univerzitní 2732/8, 301 00 Plzeň, Czech Republic*

[a)]Corresponding author: hurda@kke.zcu.cz
[b)]mata@ntc.zcu.cz

Abstract. The paper presents the research of flow instabilities in the inlet part of a centrifugal compressor channel equipped with radial inlet guide vanes. A simplified model is created and for that, a dimensional analysis of the flow is carried out. Methods of computational fluid dynamics (CFD) are employed in a parametric study, which gives basic information about the influence of dimensionless parameters influence to the flow field. Reconstruction of comprehensive measurement data from an experimental single stage compressor mounted with several stages of variable flow capacity is done for the purpose of comparison to the simplified model. Further analyses will be published later.

INTRODUCTION

The work is motivated by findings in the experimental research of centrifugal compressor stages. In the years 2013 to 2019 Howden ČKD Compressors, a Czech industrial company, have cooperated with New Technologies – Research Centre of University of West Bohemia on testing of new family of centrifugal compressor stages.

A single stage compressor with exchangeable flow part was operated in a wide range of regimes to simulate the whole range of its possible industrial applications. The reference Mach number based on intake air speed of sound and impeller blade tip speed was varied from 0.5 to 1.1. More detailed description of the machine can be found in [1, 2, 3].

After testing the sole stages with axial impeller intake flow, radial inlet guide vanes (IGV) were mounted. These are commonly used to control the compressor performance by adjusting the angle of the flow at the impeller intake. Mounting the guide vanes in a radial channel allows for much shorter distance between shaft bearings of industrial multistage machines than using an axial channel. The specific IGV mechanism used at the compressor test bed was capable of setting the chord of their symmetrical airfoil profile to an angle between -30° to 75°, measured from radial direction. A negative angle means causing the rotation of the flow in the opposite sense than the rotation of the impeller. The blades are located between stations 0 and 0b denoted in middle part of Figure 1. A frontal view of the control mechanism and prismatic blade profiles are depicted in the right part of the same Figure.

For some of the tested stages, excessive noise and performance loss occurred at certain operating conditions. The discovered reason of these issues lies in the boundary layer separation in the channel in front of the impeller.

The research has the goals set to provide generalized results and design recommendations in the end, so instead of searching for minor optimizations in the geometry of existing stages, a careful study of the phenomena is carried out. This begins with maximum possible simplifications, dimensional analysis and parametric study, which is presented in this preliminary article. In the last part of this contribution, the values of the simplified model parameters are searched for in the measured compressor stages.

19th Conference on Power System Engineering
AIP Conf. Proc. 2323, 060006-1–060006-9; https://doi.org/10.1063/5.0041454
Published by AIP Publishing. 978-0-7354-4067-8/$30.00

THE SIMPLIFIED MODEL

The model is created to be able to reproduce a flow field with boundary layer separation caused by concurrently acting pair of centrifugal forces of two superposed rotational movements of fluid. One rotational movement is bending the flow from centripetal direction behind the IGVs to centrifugal direction inside the impeller and the other is the flow rotation around machine axis caused by the IGV angle adjustment. For modeling of this phenomenon, all the features of an impeller can be dropped including blading, rotating channel walls, clearances and seals etc.

Not to introduce proprietary and complex compressor geometry (see middle part of Figure 2) in this generalized analysis, the meridional shape of the channel has been constructed from concentric half-circular arcs and straight radial elongations on both ends. This simple geometry has just three parameters – the channel width (t), radius of channel axis relative to machine axis (r_t) and the radius of the axis in the axial bend from centrifugal to centripetal flow direction (r_a). Such geometry is subject to dimensional analysis and later the computational parametric study. It is depicted in left part of Figure 1.

The purpose of the straight elongations is the elimination of CFD boundary conditions influence to the flow field in the most concerned area. The length is kept fixed in terms of multiples of the thickness value.

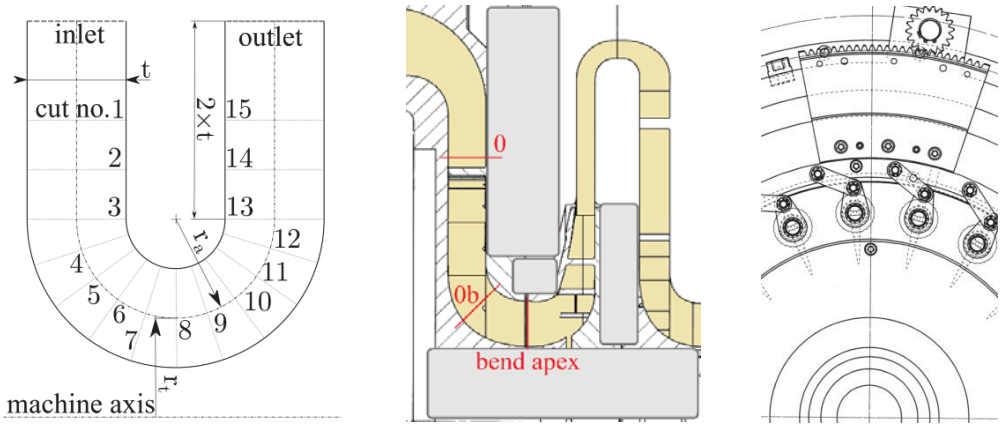

FIGURE 1. Left: Simplified model with post-processing cuts. Middle: Real compressor geometry – stage s4 with significant measuring stations (flow channel in beige; grey rectangles for censoring parts of proprietal documentation). Right: Frontal view of radial IGV control mechanism, vane profiles dotted as hidden edges. Adapted from [5].

DIMENSIONAL ANALYSIS

The simplicity of the model allows the creation of two geometrical simplexes: $T = r_t/t$ and $A = r_a/t$. Only incompressible flow cases are considered at the start of the analysis. This allows neglecting the influence of Mach number and sets the Reynolds number (Re) based on channel width (t) and bend apex flow speed magnitude (U) as the only flow parameter beside the IGV angle (ϑ).

The forces of friction and inertia are tied together with Re, but in the rotational flow, also centrifugal body forces are acting. The centrifugal force criterion can be expressed as the body force magnitude divided by the scale of centrifugal force based on already defined characteristics: U^2/t [4]. For the two rotational movements present, two criteria are defined as follows (U_a and U_t are axial and tangential components of velocity vector in the bend apex respectively). The relation to the already defined parameters A, T, ϑ is clear from equation (1).

$$Ce_a = \frac{t}{r_a} \cdot \frac{{U_a}^2}{U^2} = \frac{\cos^2 \vartheta}{A}\,[1]; \qquad Ce_t = \frac{t}{r_t} \cdot \frac{{U_t}^2}{U^2} = \frac{\sin^2 \vartheta}{T}\,[1] \tag{1}$$

Kinematic similarity should be ensured by constancy of the Strouhal number. It is expressed using the defined characteristic measures of velocity and length and a frequency measure defined by rotating flow parameters. As seen in the equations (2) below, these criteria are dependent on already defined parameters as well.

$$Sh_a = \frac{t}{U} \cdot f_a = \frac{t}{U} \cdot \frac{U_a}{\pi A t} = \frac{\cos \vartheta}{\pi A}\,[1]; \qquad Sh_t = \frac{\sin \vartheta}{\pi T}\,[1] \tag{2}$$

As all the thinkable flow cases are expected to be turbulent, the parameters of turbulence should be considered too. For the turbulence mathematical modeling approaches used in the upcoming computational study – two transport equation turbulence models – the turbulence intensity (I) is estimated and the channel width (t) is used as the hydraulic diameter. This is enough to define and prescribe the initial and boundary conditions for the modeled turbulent quantities.

The simplified model is described using 5 dimensionless parameters: A, T, ϑ, Re, I.

PARAMETRIC STUDY

An axisymmetric, quasi-2D geometry is used to simulate the steady incompressible viscous flow. As for some cases of the experimental compressor measurements the Mach number is higher than allowable for incompressible flow description, compressible flow analyses will be a part of future work. This will inevitably complicate the parametrization as further parameters will arise.

The methodology of numerical simulations is described in detail in [5]. The mesh resolution connected with proper turbulence model and wall modelling approach was tested and set. $k-\omega$ SST turbulence model is used on structured mesh of roughly 1 million of finite volume cells in the quasi-2D case allowing wall-resolved computations without the employment of wall functions.

It was discovered that when the case is converted to 3D (30° axisymmetric wedge), it loses the ability to converge well. Despite that, the flow characteristics averaged across the wedge angle remain very close to the case using just one layer of cells in the tangential direction. For precise quantitative description of the flow, 3D unsteady flow simulation would then be necessary. For the parametric study, 2D axisymmetric case is utilized.

Post-processing Techniques

The effort was made to express the coefficients of pressure (c_p) and friction (c_f) along both channel walls. The vector components of wall shear stress (τ_w) has been transformed in the curvilinear coordinates of the wall surface and treated separately to produce graphs for meridional, tangential (and prospectively transversal) parts of coefficient of friction. The dynamic pressure (in the denominator) is expressed in kinematic form and is based on the mean flow velocity in the bend apex.

$$c_p = \frac{p}{\frac{1}{2}U^2}\ [1]\ ; \quad c_f = \frac{\tau_w}{\frac{1}{2}U^2}\ [1] \tag{3}$$

To analyse flow away from the walls, several meridian-normal surface cuts were sampled to evaluate the angles of the velocity vector relative to these surfaces. The meridional angle describes the desired rotation of the flow and the transverse angle represents the disruptions and redistribution of the flow across the channel.

It the torus shaped channel, the flow area varies a lot along the channel length and also across the channel width. Using the geometry of the channel, the volume flow rate can be normalized by the locally disponible flow area to get the information about how much more or less fluid is travelling through a certain spot then compared to an evenly distributed flow across the channel. Figure 6 uses such normalized flow rate quantity noted as $d\dot{V}/dS$.

The walls of the channel are called inner and outer from the point of view of the axial bend, so the wall closer to the machine axis is called outer. This may not mislead the reader.

Flow Angle Influence

The flow angle ϑ was varied from 0° to 60° by 5°, other parameters were fixed to: $A = 1$, $T = 1$, $Re = 10^6$, $I = 3\%$. The most important feature of the flow is the separation of boundary layer and adjacent recirculation zone emerging at the outer wall after an increase of ϑ above 40°, as seen in Figure 2. Less interesting curves are omitted in Figure 3 showing the pressure and friction coefficients. X is the channel wall relative length from inlet to outlet (including straight radial parts). Secondary horizontal axis denotes the bend angle, its ticks conform with cuts 3-10 as noted in left part of Figure 1.

The similar backflow zone is present in the aft part of the bend at the inner wall in all the cases discussed here. It probably does not have a significant relation to the flow in a real machine as it happens in the region far inside the impeller where the velocity field will be significantly different.

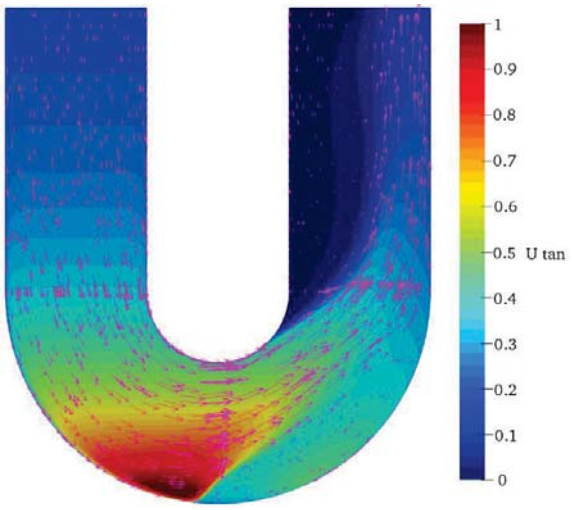

FIGURE 2. Velocity field for 45°case of flow angle influence study. Adapted from [5].

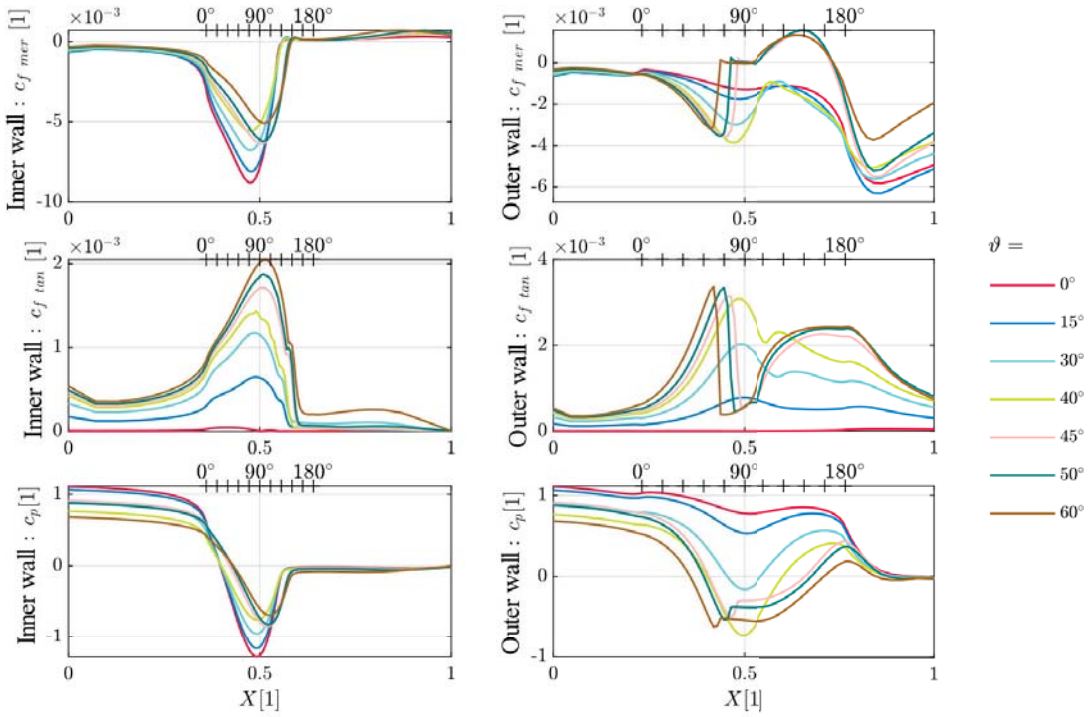

FIGURE 3. Coefficients of friction (meridional and tangential) and pressure at the channel walls for variable flow angle. Adapted from [5].

On the other hand, the ring vortex on the outer side blocks the flow quite effectively, plus it suppresses the tangential velocity component inside itself, so the flow angle becomes much more uneven than in cases without this vortex.

Channel Shape Influence

The adjustment of geometrical parameters A and T was done together. Values of 0.8, 1, and 1.2 were permuted to produce 9 cases. From the results of previous study, the value of ϑ was fixed to 45° and the influence of the geometry adjustments to the flow separation from the outer wall has been observed.

The discussed changes in geometry did not suppress the recirculation at the outer channel wall. Smaller A causes sooner separation at the inner side and this influences also the location of the reattachment of the boundary layer to the outer wall. Surprisingly, T has just a quantitative influence on the coefficients' extreme values, which relates to a different shape of function of the flow area along the bend. The ratio of the flow area at the beginning of the bend to the flow area in its apex is equal to $(T + A)/T$, which means the acceleration of the fluid in the first half of the bend and the deceleration in the second half is more intense for higher values of T.

The data commeted above are visible in Figure 4. Due to the variable length of the bends, the straight radial parts have been cut off the graphs and the remains has been fitted in the polar coordinate system of the bend.

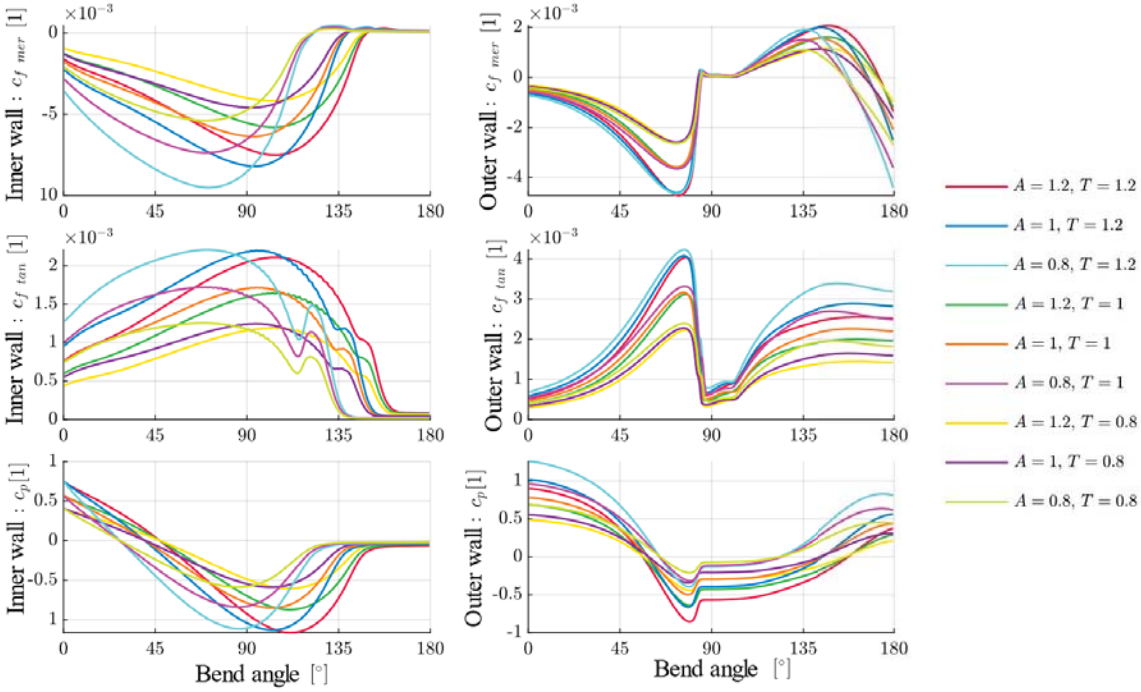

FIGURE 4. Coefficients of friction (meridional and tangential) and pressure at the channel walls for variable channel geometry. Adapted from [5].

Reynolds Number Influence

The base case of $A = 1$, $T = 1$, $\vartheta = 45°$ was tested. The base value of the Reynolds number of 10^6 was shifted by a half decimal order up to $5 \cdot 10^6$ and down to $5 \cdot 10^5$. None of the cases exhibited a diminishing of the recirculating flow at the outer wall.

The shift upwards caused just minor qualitative changes while the shift downwards has caused sooner separation of the flow from the inner wall, which happens near bend apex, even without the support of adverse pressure gradient commonly generated in the aft part of the channel. This leads to much less favorable distribution of tangential velocity across the channel right behind the apex.

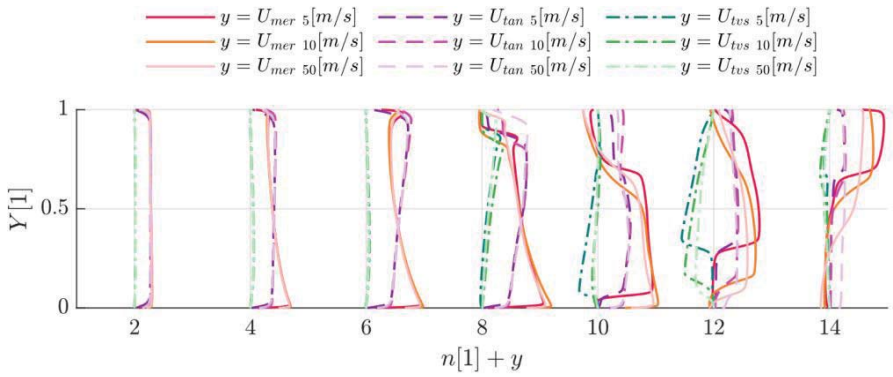

FIGURE 5. Profiles of velocity components for variable Reynolds number. (*n* equals the cut number from Figure 1-left.) Adapted from [5].

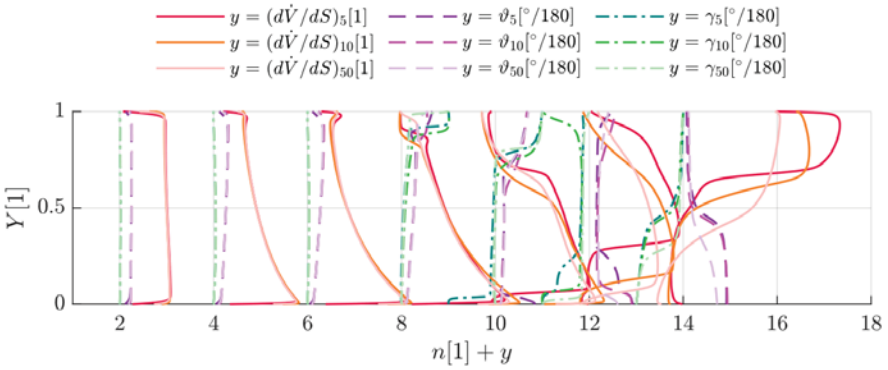

FIGURE 6. Profiles of normalized flow rate, tangential velocity angle and transverse velocity angle. (*n* equals the cut number from Figure 1-left.) Adapted from [5].

RELATED REAL COMPRESSOR STAGES PARAMETERS

A total of four stages with impeller outlet diameter of 440 mm were measured thoroughly with IGVs [6]. Only two of them are chosen for the initiation of the analysis. The higher capacity stage is designated 's2' and has an impeller outlet width ratio of 0.0775; the impeller has twisted blades with integrated inducer. The second stage is designated 's4' and has an impeller outlet width ratio of 0.0425, the impeller has prismatic backswept blades without inducer. This stage is depicted in middle part of Figure 2.

The channels in the real machines have variable channel width and variable curvature of the bends, so the upcoming values of geometrical simplexes are just an approximation. The care taken to represent the real geometry by earlier presented simplified model parameters is biased towards the part of the channel in front of the impeller rather than in the impeller, where the simplified model results will be imprecise anyway. The approximated geometrical parameters are:

- Stage s2: $A = 0.76;\ T = 1.49$
- Stage s4: $A = 1.80;\ T = 2.53$

Reynolds and Mach Number Calculation from Measured Data

A challenge to express the Re and Ma in the desired location of the flow channel required a sophisticated use of standard measurement data evaluation procedures. A complete measuring station ('0') was placed in front of the IGVs, and only static pressure taps were present only on the outer wall of the channel behind IGVs. These were not located in the bend apex, but after 45° of the turn (measuring station '0b').

It was attempted to calculate the actual angle of the flow. That required the approximation of total pressure (p_c) and total temperature (T_c) in the measuring station 0b. First, the pressure loss of the IGVs was expressed from the static pressures (p_s) and a guess of the dynamic pressure (p_d) change (based on the flow area ratio assuming the rotation of the flow with zero deviation from IGV angle setting):

$$\Delta p_{IGV} = (p_{s0} - p_{s0b}) - (p_{d0} - p_{d0b}) = (p_{s0} - p_{s0b}) - p_{d0}\left(1 - \frac{A_0}{A_{0b} \cdot \sin(90° - \vartheta)}\right) \quad (4)$$

This pressure loss was subtracted from the total pressure in front of IGVs to approximate the total pressure in station 0b. Total temperature in 0b was calculated for an isenthalpic state change from p_{c0} to p_{c0b}. The calculation of flow angle is based on the meridional velocity expression from mass flow rate and total velocity magnitude based on total to static enthalpy difference. The procedure is iterative due to reciprocal dependence of fluid static state on the flow velocity and was briefly explained in [7]. The algorithm is too sensitive, and the limitations of the approximations made earlier together with questionable accuracy of static pressure taps measurement in station 0b, causes it to be inapplicable for calculation of flow angle deviation behind IGVs.

Instead, the above described procedure of approximating T_{c0b} was used to calculate the flow velocity with an assumption of zero flow angle deviation from IGV setting. This was achieved by using the approximated T_{c0b} and the measured p_{s0b} and setting the station flow area as its projection to the rotating flow direction $A_{0b}^{fictional} = A_{0b}^{actual} \cdot \sin(90° - \vartheta)$.

The determination of the working fluid state in station 0b allowed the expression of fluid state in the bend apex. It has been done by simple extrapolation of the total state of fluid and recalculation of the static state for the respective flow area change. Then, the flow velocity, kinematic viscosity and speed of sound (w, ν, a respectively) may have been determined in order to express $Re = w \cdot t/\nu$ and $Ma = w/a$ values corresponding to the CFD parametric study.

RESULTS

Figure 7 sums up the results. Though the inputs of criterion calculations as viscosity or density vary strongly and partly randomly, the curves of Re and Ma are close to linear dependency on mass flow rate and flow angle – the compressor map branches groups together by angle in the $\dot{m} - Re$ space. This dependency could effectively reduce the number of cases of further parametric study, if just one gas as working fluid needed to be considered. The compressors often work with gases of substantially different properties. The linear coefficients of presented curves would differ for a different gas than atmospheric air, which was used on the test bed.

Mach number is low enough (<0.3) for many cases to be studied as incompressible, but not for all of them. The difference between total and static state parameters can be observed well below the mentioned limit.

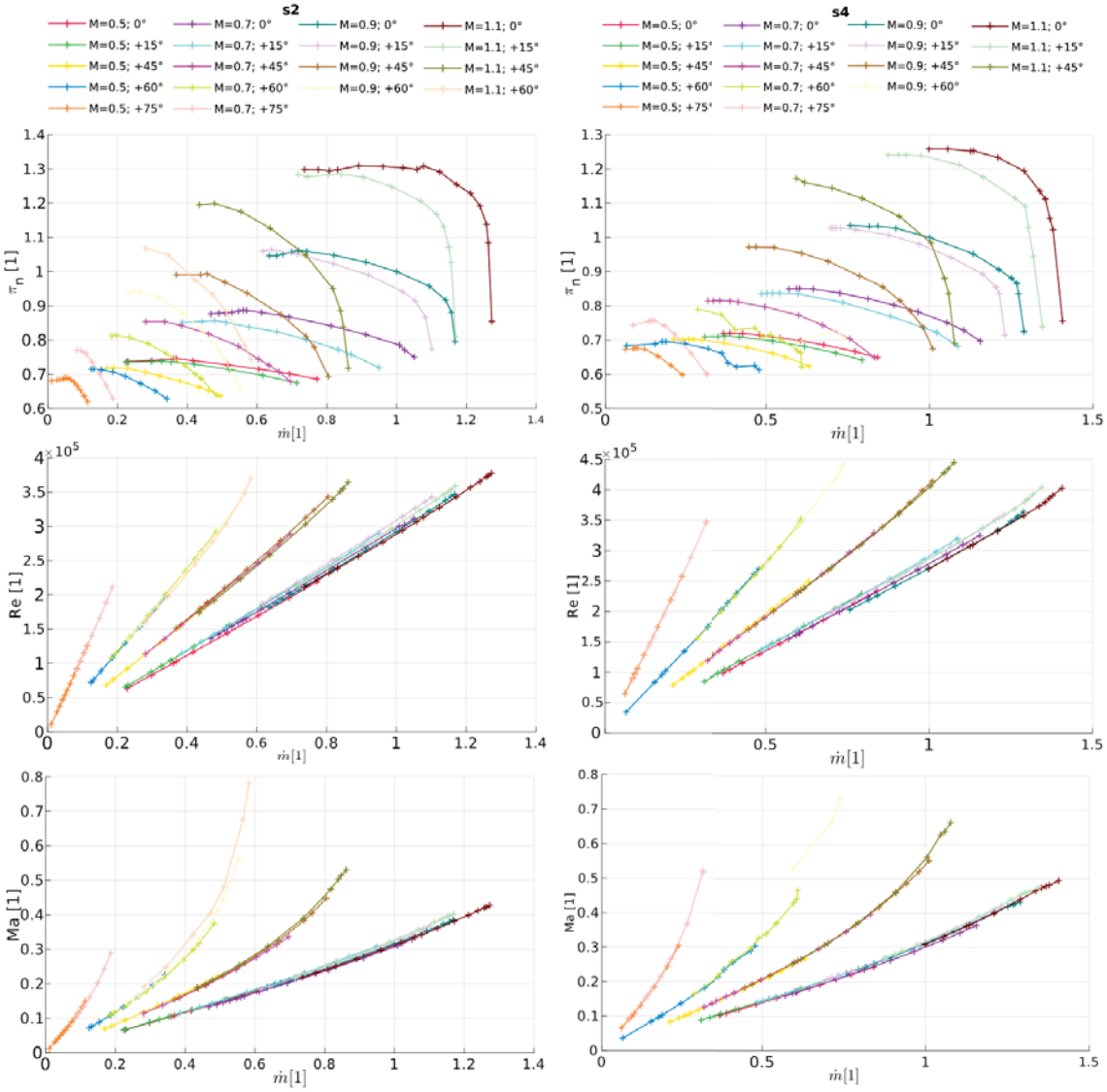

FIGURE 7. Normalized pressure ratio (top), inlet bend apex Reynolds number (middle) and Mach number (bottom) versus normalized flow rate for stages s2 (left) and s4 (right).

CONCLUSION

The First part of a vast analysis is presented. The studied influence of rotating flow behavior in the inlet channel of a centrifugal compressor is successfully reduced to relatively simple parametric study using approximative geometrical model and dimensional analysis. The methodology of the parametric study is built and proved.

The parametric study will continue with further cases in the range of parameters, where qualitative changes were observed. The parameters will also be shifted to values according to real compressor stages, for which the results can be confronted with measurement data. The methods for calculating the comparable values from measured data were presented too. Then the effects of separate flow features can be linked to departures of the compressor performance parameters.

ACKNOWLEDGMENTS

The authors thank to Howden ČKD Compressors for the courtesy of publication of research based on their documentation and measurement data.

This work was financially supported by student project SGS-2019-021 (Improving the efficiency, reliability and service life of power machines and equipment 5).

REFERENCES

1. T. Syka; R. Matas; O. Luňáček. “Numerical and Experimental Modelling of the Radial Compressor Stage,” in *AIP Conference Proceedings 1745*, (American Institute of Physics, Melville, NY, 2016), 020059.
2. T. Syka; R. Matas; O. Luňáček. “Numerical and experimental modelling of the centrifugal compressor stage – setting the model of impellers with 2D blades,” in *EPJ Web of Conferences, 143* (EDP Sciences, Les Ulis, France, 2017), 02073.
3. R. Matas; L. Hurda and J, Mráz. “Shrnutí výsledků výzkumu a vývoje radiálních kompresorových stupňů na zkušebním kompresoru DARINA IV,” in *Turbostroje 2019* (Techsoft Engineering, Prague, 2019, in Czech).
4. S. M. Gorlin, and I. I. Slezinger, *Wind Tunnels and Their Instrumentation*. (Nauka, Moscow, 1964, Translation: Israel Program for Scientific Translations, Jerusalem, 1966).
5. L. Hurda, “Numerical Analysis of Fluid Flow in the Intake Channel of a Centrifugal Compressor Stage with Radial Inlet Guide Vanes,” Ph.D. thesis intermediate report, University of West Bohemia, 2020, (in Czech).
6. Howden ČKD Compressors (compressor test bed documentation and measurement data).
7. L. Hurda and R. Matas. “Radial Compressor Test Data Processing with Real Gas Equation of State,” in *AIP Conference Proceedings 2189*. (American Institute of Physics, Melville, NY, 2019). ISBN 978-0-7354-1936-0, ISSN 0094-243X.